

1
2
3
4
5
6
7
8
9
10
11
12
13
14
15
16
17
18
19
20
21
22
23
24
25
26
27
28
29
30
31
32
33
34
35
36
37
38
39
40
41
42
43
44
45
46
47
48
49
50
51
52
53
54
55
56
57
58
59
60
61
62
63
64
65

1 **Title:**

2 Allograft Selection for Transepiphyseal Tumor Resection around the Knee Using 3-Dimensional
3 Surface Registration

4 **Abbreviated Title**

5 Allograft Selection Using Surface Registration

6 **Authors:**

7 Habib Bou Sleiman¹

8 Lucas E. Ritacco²

9 Luis Aponte-Tinao²

10 Domingo L. Muscolo²

11 Lutz-Peter Nolte¹

12 Mauricio Reyes¹

13

14 **Affiliations:**

15 1. Institute for Surgical Technology and Biomechanics, University of Bern, Stauffacherstrasse
16 78, CH-3014, Switzerland

17 2. Hospital Italiano de Buenos Aires, Gascon 450 Buenos Aires, Argentina

18

19 **Corresponding Author:**

20 Habib Bou Sleiman

21 Phone: +41 (0) 31 631 59 48

22 Facsimile: +41 (0) 31 631 59 60

23 e-mail: habib.bousleiman@istb.unibe.ch

Abstract:

Transepiphyseal tumor resection is a common surgical procedure in patients with malignant bone tumors. The aim of this study is to develop and validate a computer-assisted method for selecting the most appropriate allograft from a cadaver bone bank. Fifty tibiae and femora were 3D reconstructed from CT (computed tomography) images. A transepiphyseal resection was applied to all of them in a virtual environment. A tool was developed and evaluated that compares each metaphyseal piece against all other bones in the data bank. This is done through a template matching process, where the template is extracted from the contralateral healthy bone of the same patient. The method was validated using surface distance metrics and statistical tests comparing it against manual methods. The developed algorithm was able to accurately detect the bone segment that best matches the patient's anatomy. The automatic method showed improvement over the manual counterpart. The proposed method also substantially reduced computation time when compared to state-of-the-art methods as well as the manual selection. Our findings suggest that the accuracy, robustness, and speed of the developed method are suitable for clinical trials and that it can be readily applied for preoperative allograft selection.

Key Terms

Orthopaedic oncology, Tumor resection, Allograft selection, Surface registration, Computer-assisted surgery

1
2
3
4 **1 Abbreviations, Symbols, and Terminology**

- 5
6 2 b_i i^{th} bone from the databank
7
8
9 3 cc Convergence criterion of ICP
10
11 4 CT Computed tomography
12
13
14 5 DB Databank
15
16 6 HSD Hausdorff surface distance (mm)
17
18
19 7 ICP Iterative closest point
20
21 8 $maxIt$ Maximum number of iterations for ICP
22
23
24 9 MRI Magnetic resonance imaging
25
26 10 MSD Mean surface distance (mm)
27
28
29 11 n Number of surface points of the search template
30
31 12 p_b Point on the bone from databank
32
33
34 13 p_s Point on the search template
35
36 14 s Search template
37
38 15 s_T Transformed search template
39
40
41 16 SD Standard deviation
42
43 17 **T, TR** Transformation matrix
44
45
46 18
47
48 19
49
50 20
51
52
53 21
54
55 22
56
57
58 23
59
60
61
62
63
64
65

1 Introduction

2 Transepiphyseal resection and consecutive reconstruction is a common surgical procedure in a
3 wide number of patients suffering from malignant bone tumors. In this specific surgical scenario,
4 the bone is cut in a way to preserve the epiphysis (Figure 1d), and therefore an intercalary
5 implant is required for the reconstruction. Various reconstruction methods exist, and the
6 applicability of each of the methods is a strictly case-dependent decision.¹⁷ Biological
7 reconstructions in great defects caused by transepiphyseal tumor resection around the knee is a
8 major challenge of oncologic orthopaedics. Clinical reports suggest that those defects can be
9 repaired using bone allografts to preserve the long term bone stock and limb
10 functionality.^{12,15,16,17,22} Matejovsky *et al.*¹² and Ramseier *et al.*²² further support and promote
11 the use of allografts as opposed to prosthetic intercalary implants, especially in younger patients.
12 This was based on the long-term follow-up of their patients over time periods of several years.
13 Moreover, Bielack *et al.*,² Matejovsky *et al.*,¹² and Paulussen *et al.*²⁰ indicated that the tibia is a
14 site presenting a high incidence of bone malignancies. A good allograft also facilitates and
15 enhances the fitting process of the fixation plate(s). Furthermore, optimal handling of the bone
16 bank ensures minimal loss of the usually scarce cadaver bone stock.

17
18 At present, we are not aware of any published automatic method able to select the best allograft
19 around the knee from a virtual bone bank system based on shape analysis. However, recent
20 studies demonstrated that a virtual model is a potential predictor to select the adequate allograft
21 in a preoperative planning environment.¹⁹ Furthermore, shape matching is the chief method to be
22 considered when a proper allograft is to be selected.^{6,7,18,19}

1 This work is an extension of our previous work⁴ where we presented preliminary results on
2 automatic allograft selection. However, the method presented several limitations. In particular,
3 the degrees of freedom of the spatial search were only limited to the cranio-caudal direction,
4 whereas no consideration to the remaining rotation and orientation parameters was regarded.
5 Furthermore, the size of the validation dataset was reduced to ten patient computed tomography
6 (CT) images, from which low resolution surface models of the femur were generated.
7 Nevertheless, the obtained results were satisfactory, and brought forward a series of open-ended
8 questions to be further investigated, relating to both the clinical and technical aspects of the
9 method.

11 This study was also inspired by the findings of Ritacco *et al.*,²³ Schmidt *et al.*,²⁴ and Seiler *et*
12 *al.*,²⁵ where it was shown that a pattern of symmetry between the contralateral lower limbs of the
13 same subject does in fact exist. The search for the optimal allograft is automatically carried out
14 through a databank of cadaver bones, in which the search is routinely performed manually.^{14,18,23}
15 In a similar context, Paul *et al.*^{18,19} presented methods for the selection of massive bony
16 allografts, in particular hemipelvic allografts. They employ either manual two-dimensional
17 outline comparison or automatic three-dimensional image registration approaches in order to find
18 the best donor. They also compare the two methods and show evidence that the registration
19 method outperforms the planar outline matching. However, they consider the pelvis as a whole
20 and do not discuss the problem of selecting an allograft for a localized region. They also do not
21 simulate real clinical scenarios as they consider that the original anatomy of the pelvis is known
22 beforehand. Towards the end of their discussion, they propose to rely on symmetry in order to
23 recover information about the original anatomy of the patient at the tumor site.

1
2
3
4 1
5
6 2 This paper presents a novel computer-assisted method for the selection of the allograft that best
7
8
9 3 matches the patient specific anatomy for transepiphyseal tumor resection around the knee. This
10
11 4 work integrates concepts presented elsewhere,^{1,4,23,24,25} together with sound clinical aims and a
12
13
14 5 more elaborate and comprehensive methodology, into an automatic system that provides the
15
16 6 orthopaedic surgeon with a relatively fast and accurate solution to the problem of selecting a
17
18 7 good allograft. The functional outcome of the surgery is thus enhanced and the durability of the
19
20 8 implant extended.^{12,15,16,17,22} The method adds to the recent research¹⁹ the capability of selecting
21
22 9 allografts for specific regions of the bone while taking into account that the presence of a tumor
23
24
25 10 alters the original shape of the recipient bone.
26
27
28
29
30

31 12 This study aims to first assess the ability of the presented method to automatically select an
32
33 13 adequately matching allograft. It also aims to explore whether it yields comparable or better
34
35 14 results than those obtained by the manual method, and if its reproducibility is sufficiently reliable
36
37
38 15 for clinical use.
39
40
41
42

43 17 **HERE GOES FIGURE 1**
44
45
46
47

48 19 **Methods**

49
50 20 The method proposed in this article takes advantage of the aforementioned concept of symmetry
51
52 21 in order to reconstruct the original shape of a diseased portion of the bone. A template
53
54 22 corresponding to the location of the tumor is extracted from the patient's healthy contralateral
55
56
57 23 bone. An iterative three-dimensional template matching process is then applied through the
58
59
60
61
62
63
64
65

1 virtual cadaver bone databank in order to locate bone portions that resemble the template in
2 terms of both morphology and scale. System testing and validation was carried out by simulating
3 clinical cases from the available data.

4
5 The method presented herein was developed, tested, and validated using a set of 50 patient CT
6 images of the lower limbs (varying image parameters and scanners). The bones were semi-
7 automatically segmented using Amira® (Visage Imaging, Inc., San Diego, CA, USA), and stored
8 in the form of surface point models and surface meshes (vertices per sample – tibiae: 42,004;
9 femora: 58,837). This data is regarded as a digitally stored cadaver bone databank, in analogy to
10 the one presented in Ritacco *et al.*²³ From this point onward, we will be referring to those bones
11 as cadaver bones.

12
13 The overall application of this method can be briefly described as follows: having a diseased
14 bone, one can use the hereby presented tool in order to find amongst a set of healthy ipsilateral
15 cadaver bones, the allograft that best matches the anatomy of the part to be resected. Knowledge
16 about the original shape of that section is obtained from the contralateral bone of the same
17 patient. This is achieved by first pre-registering the healthy contralateral bone to the diseased
18 bone and manually cutting the part that corresponds to the location of the tumor. The processing
19 pipeline therefore consists of the following steps, which are illustrated in Figure 1:

- 20
21 1) Acquisition of the CT images and segmentation of the patient's bones and tumor
22 (Figure 1a-1c)

- 1
- 2
- 3
- 4 1 2) Virtually cutting out a part of the healthy contralateral bone that corresponds to the
- 5
- 6 2 location of the tumor (Figure 1d)
- 7
- 8
- 9 3 3) Automatic registration of the template with all bones in the databank and storing
- 10
- 11 4 measured distance metrics (Figure 1f)
- 12
- 13
- 14 5 4) Automatic selection of the closest (or few closest) match(es) from the databank
- 15
- 16 6 (Figure 1f)
- 17
- 18
- 19 7 5) Using the boundaries of the registered template to outline the physical cutting planes
- 20
- 21 8 on the selected bone and extract the allograft
- 22
- 23
- 24 9

25

26 10 As mentioned earlier, the original anatomy of the diseased bone is extracted from the patient's

27

28 11 healthy contralateral limb and used as a template to guide the search within the databank of

29

30 12 cadaver bones. This is illustrated in the form of a pseudo-code in Algorithm 1. For each cadaver

31

32 13 bone in the databank (line 2), the algorithm applies an iterative closest point¹ (ICP)-based

33

34 14 registration on the point clouds of the template and the bone itself in order to find the transform

35

36 15 that minimizes the difference between the two surfaces (lines 4-7). This is done in an iterative

37

38 16 fashion and only stops when a certain convergence criterion ($cc = 0.001mm$, line 8) is met, or

39

40 17 when the number of iterations exceeds a preset value ($maxIt = 200$, line 8). Surface distance

41

42 18 metrics are measured and stored for further processing (line 7). The rigid transformation is then

43

44 19 applied to the template in order to place it in the best fitting location and orientation. This

45

46 20 process is repeated until all bones in the databank are examined. An identity transformation is

47

48 21 used to initialize the registration in order to avoid biased results. This could be on the expense of

49

50 22 falling into local minima, but with the advantage of being able to find any matching bone

51

52

53

54

55

56

57

58

59

60

61

62

63

64

65

1 segment along the potential donor bones and not only those close to the anatomical region of the
2
3
4
5
6
7
8
9
10
11
12
13
14
15
16
17
18
19
20
21
22
23
24
25
26
27
28
29
30
31
32
33
34
35
36
37
38
39
40
41
42
43
44
45
46
47
48
49
50
51
52
53
54
55
56
57
58
59
60
61
62
63
64
65

1 segment along the potential donor bones and not only those close to the anatomical region of the
2 tumor.

3
4 At this stage, each bone in the databank is represented by the minimum surface distance metric
5 between the bone itself and the best fit of the template. Since the goal is to find the closest global
6 match, one or more closely matching donors can be selected (lines 16-17), thus giving the
7 surgeon one-to-few possibilities to choose from.

8 9 **HERE GOES ALGORITHM 1**

10 11 **Validation Protocol**

12 *Simulated Clinical Cases*

13 A testing application was developed in order to assess the robustness of the proposed method and
14 evaluate its possibility to be applied in a clinical setup. In every test iteration, the tool considers
15 one dataset as a clinical case while using the remaining bones as the cadaver bones – the dataset
16 taken as a clinical case is also included in the databank and used as a control sample, or what is
17 referred to in Paul *et al.*^{18,19} as trap graft. A clinical case consists of an assumingly diseased left
18 bone, and its healthy contralateral counterpart belonging to the same patient. For every case, the
19 template is cut out of the right-side bone and then fed to the template matching algorithm
20 described earlier whose role is to find, within the bone databank, the bony part that best matches
21 the shape of the template. The collective results of the validation experiments are listed in the
22 following section.

1 Corresponding points between the template in its final position and the databank bone are
 2 efficiently computed by applying a space dividing *kd*-tree data structure to the complete bone,
 3 and then selecting the closest points to those of the template. Surface distance metrics that were
 4 used for the validation of this method are the mean surface distance (*MSD*) and the Hausdorff
 5 surface distance (*HSD*). The former consists of the average value of the individual Euclidean
 6 distances between corresponding surface points. It provides information about the overall global
 7 similarity between the donor and the recipient. The latter is the largest amongst the individual
 8 Euclidean distances and it indicates the largest possible distance between the two surfaces. More
 9 formally, the distance metrics can be written as follows,

$$MSD(s, b) = \frac{1}{n} \sum_{k=1}^n \|p_{sk} - p_{bk}\|, \quad (1)$$

$$HSD(s, b) = \max\{\|p_{sk} - p_{bk}\| \mid k = 1, \dots, n\}, \quad (2)$$

15 where k is the index of the search template point, n the number of template surface points, and
 16 $\|p_{sk} - p_{bk}\|$ is the three-dimensional Euclidean distance between the k^{th} template point and its
 17 corresponding point on the surface of the examined bone. In Equation 1 and Equation 2, s and b
 18 refer to the template and the cadaver bone, respectively.

20 *Performance Assessment*

21 A subset of ten clinical cases was used to evaluate the performance of the method relative to that
 22 of the manual approach. Two observers were asked to manually choose the best three matches
 23 for each template. Manual search was carried out using a computer interface with an interactive
 24 virtual environment within Mimics® (Materialise NV, Leuven, Belgium). Each result was

1 individually scored. The Automatic method was applied in parallel and the best three matches for
2 every template were noted and scored. The scoring system is based on a visual assessment of the
3 fit of the allograft with particular attention to the overlap at the boundaries especially at the sites
4 where a fixation plate would be placed.

5
6 Fisher's exact test was used to identify differences in the capability of both methods to detect the
7 contralateral or trap graft (The Chi-squared test was not chosen because the expected frequencies
8 in the contingency tables were smaller than 5). A significance level of 0.05 was chosen for all
9 tests.

10

11 Agreement between both methods in choosing the three best matching allografts (with no
12 consideration to their order) was assessed using Cohen's kappa.⁵ Using this result, it is possible
13 to conclude about whether or not both methods are able to yield similar results.

14

15 Furthermore, Cohen's kappa was computed for the automatic method when applied four times on
16 the same datasets. This measure would quantify the reproducibility of the method. Similarly, the
17 reproducibility of the manual method was assessed by measuring the Cohen's kappa for the two
18 observers.

19

20 **Results**

21 In this section, the results of the validation protocol of the presented method are listed. The
22 template matching algorithm was tested on a computer with a 32 bit architecture, 3.00 GHz
23 Intel® Core™ 2 Duo CPU, and 3.25 GB of random access memory. The algorithm never failed

1 to run or fell into numerical errors. Comparing a template to a single bone from the databank
2 took 1.73 ± 0.62 seconds (*mean* \pm *SD*). These figures include the time to build the *kd*-tree
3 whenever point correspondences are required. An overhead time of loading the database into
4 memory and processing of the images is to be added, however this can be done offline and is not
5 different than that done in the manual method. Convergence of the iterative algorithm was
6 mainly constrained by the preset convergence criterion. For the 50 x 50 comparisons, $97.24 \pm$
7 27.96 iterations were needed. Only three comparisons out of the total of 2,500 went over the
8 limit of number of iterations.

9
10 In terms of surface distances, one would expect the best obtained match to be part of the
11 contralateral bone of the same subject. This is due to the high similarity in the original
12 morphology of the left and right sides of the patient. This was confirmed by the obtained results
13 where an errorless classification was achieved. The control samples are therefore highlighted by
14 the diagonals in Figure 2, where the lowest *MSD* values were recorded. A similar diagonal
15 pattern is demonstrated for the Hausdorff distance measurements.

16
17 **HERE GOES FIGURE 2**

18
19 The control samples can be considered as a further validation parameter, since clinically, the
20 allograft must mimic the shape of the resected region as closely as possible, and therefore the
21 template must match the shape of the missing part. The values occurring on the diagonals of the
22 tables in Figure 2 are $0.62 \pm 0.0066\text{mm}$ (*mean* \pm *SD*) in the case of *MSD*, whereas the *HSD*
23 measurements are $2.30 \pm 0.76\text{mm}$.

1
2
3
4 1
5
6 2 Figure 3 shows three-dimensional views of the results for the best match, the second best, and
7
8
9 3 the worst for two different simulated clinical cases (i.e., two different patients). Surface distance
10
11 4 is illustrated in the form of color-coded surface maps.
12
13
14 5

15
16 6 **HERE GOES FIGURE 3**
17
18
19 7

20
21 8 Tests comparing the performance of the proposed method to its manual counterpart were carried
22
23
24 9 out on a subset of ten simulated clinical cases. Twenty manual (10 detections per observer) and
25
26 10 twenty automatic detections were carried out in total. It took the observer on the average 12
27
28
29 11 minutes per template to manually search through the databank and give a score for each bone.
30
31 12 The automatic method was able to correctly detect the symmetric template in all of the cases.
32
33
34 13 The observers carrying out the process manually managed to correctly classify the trap graft in
35
36 14 only 12 out of the 20 cases. Fisher's exact test proved an improvement of the automatic method
37
38 15 over the manual approach ($p = 0.002$).
39
40

41 16
42
43 17 Cohen's kappa tests resulted in a value of 0.73 (95% CI: 0.63 to 0.83), indicating an
44
45 18 intraobserver agreement that is not accidental.¹¹ The two methods were therefore yielding
46
47
48 19 comparable results in terms of choosing the best three matches.
49

50 20
51
52
53 21 Reproducibility tests of the automatic method were carried out by applying the algorithm four
54
55 22 times on the same datasets. In all cases, the algorithm converged to the exact same solution
56
57
58
59
60
61
62
63
64
65

1 yielding a kappa value of 1.0 (95% CI: 1.0 to 1.0). Reproducibility of the manual method, or
2 agreement between the two observers, resulted in a kappa of 0.79 (95% CI: 0.67 to 0.91).

3 4 **Discussion**

5 In this paper we presented a novel computer-aided method for the automatic selection of the
6 donor allograft that best fits the patient-specific anatomy from a given virtual databank of
7 cadaver bones. The method is able to speed-up and enhance the current state-of-the-art that is
8 employed in the clinical setup - a rather time-consuming and error-prone manual approach. A
9 specific application was considered, namely, transepiphyseal tumor resection around the knee.
10 Patient-specific anatomy is extracted from the healthy contralateral limb of the same
11 individual.^{23,24,25}

12
13 A thorough validation of the method was presented. Two distance metrics were presented and
14 used in this paper, in particular, the mean surface distance (*MSD*) and the Hausdorff surface
15 distance (*HSD*). The *HSD* metric, as well as the location of the region presenting the largest
16 distance, are clinically relevant since they indicate whether or not the use of the particular
17 allograft and the proper fitting of the fixation plate(s) is feasible.

18
19 Tests assessing the performance of the automatic method and comparing it to that of the manual
20 method were as well carried out. The automatic method outperformed its manual counterpart in
21 terms of detecting the contralateral bone, while maintaining a substantial agreement with the
22 observers' choices of the best three matches. The presented method showed higher
23 reproducibility than that measured for the experts.

1
2
3
4
5
6
7
8
9
10
11
12
13
14
15
16
17
18
19
20
21
22
23
24
25
26
27
28
29
30
31
32
33
34
35
36
37
38
39
40
41
42
43
44
45
46
47
48
49
50
51
52
53
54
55
56
57
58
59
60
61
62
63
64
65

1

2 The method can easily be extended to test different surgical scenarios such as epiphyseal,
3 unicondylar, and bicondylar resections. Such scenarios might require intraarticular
4 reconstructions where the cartilageneous tissue has to be considered. In such cases, and since CT
5 does not provide adequate contrast in soft tissues, magnetic resonance images (MRI) can be used
6 to complement the data acquisition system. Furthermore, and in order to circumvent the common
7 shortage in donor bones, the search can be applied across dissimilar bones. For instance, a part of
8 the femur can be grafted in the patient's tibia as long as it presents adequate morphology. We
9 have plans to proceed with our research direction and further investigate those topics.

10

11 Computed tomography - and also MR - images are routinely used to determine the tumor
12 resection margins. Given the current resolution of typical images, 3D segmentations and
13 reconstructions usually offer high-quality surface models that are adequate for further
14 processing. Furthermore, the data used in the experiments of Bou Sleiman *et al.*⁴ was represented
15 point models of a lower resolution (almost half the current resolution), and the results were
16 nonetheless satisfactory. The results shown in the previous section support our initial hypothesis
17 that an automatic 3-dimensional mesh-based template matching algorithm could perform better
18 than the state-of-the-art automatic and manual techniques. The presented computer-assisted
19 method proved to be faster than the manual allograft selection and other reported approaches.^{18,19}
20 When compared to the manual search, a significant improvement was recorded while
21 maintaining a solid agreement between the expert's opinion and the outcome of the algorithm.
22 Due to its mathematically stable nature, our method proved to be highly reproducible. Moreover,
23 the algorithm did not fail to converge in any of the tested cases, and it yielded superior results to

1 those obtained by the manual method. We therefore conclude that our method is based on
2 reliable data and is accurate enough for clinical use.

3
4 The iterative closest point algorithm used in this work faces the inherent limitation of possibly
5 falling into local minima, which could diverge the results from the sought solution. However, the
6 results of our tests showed a good immunity of our method against these pitfalls. We are also
7 aware that a good fit of the edges of the allograft is of higher importance than an overall good fit.
8 We plan to investigate a weighted-ICP method in which the importance of the edges is
9 emphasized by correspondingly weighting the vertices of the surface models.

10
11 Legal, ethical, and logistic issues are usually faced when a clinical technique requires the
12 postmortem collection of organs. Nevertheless, our clinical partners have facilitated access to
13 organ donation as the country they operate in has already adopted an opt-out presumed consent
14 donation system. Seven other countries in Latin America share the same donation laws.¹³
15 Furthermore, bone banks collecting bones from donors who have agreed to sign an informed
16 consent is currently part of the healthcare standards in several countries worldwide.^{6,7,9,10}

17
18 In our initial assumption, we rely on symmetry between the right and left side of the patient in
19 order to generate the search templates. Additional methods can also be investigated, for instance
20 in the cases where there is a clear dissimilarity between the two limbs. Three-dimensional
21 surface reconstruction and prediction methods, especially those based on a statistical shape
22 model,^{3,8,21} are also capable of providing valuable information about the original shape of the

1 operated bone. The large database of segmented long bones developed at our institute makes this
2 kind of experiments feasible for future studies.

3
4 Our approach however searches for the best donor based on global surface characteristics.
5 Nevertheless, displaying color-coded maps of local surface distances, as well as providing the
6 surgeon with a choice of more than one candidate donor renders the tool more flexible and leaves
7 the final decision to the expert.

8 9 **Acknowledgment**

10 This work was carried out within the frame of the National Center of Competence in Research,
11 Computer-Aided and Image-Guided Medical Interventions (NCCR Co-Me), supported by the
12 funds of the Swiss National Science Foundation (SNSF).

13 14 **References**

- 15 1. Besl, P. J. and N. D. McKay. A Method for Registration of 3-D Shapes. *IEEE Trans. PAMI*
16 14(2):239-56, 1992.
- 17 2. Bielack S., B. Kempf-Bielack, D. Schwenzer, T. Birkfellner, G. Delling, V. Ewerbeck, *et al.*
18 Neoadjuvant therapy for localized osteosarcoma of extremities. Results from the Cooperative
19 osteosarcoma study group COSS of 925 patients. *Klin. Padiatr.* 211(4):260-70, 1999.
- 20 3. Blanz V., A. Mehl, T. Vetter, and H. P. Seidel. A statistical method for robust 3D surface
21 reconstruction from sparse data. In: Proc. 2nd Int. Symp. 3D Data Processing, Visualization, and
22 Transmission, 2004, pp. 293-300.

- 1 4. Bou Sleiman H., L. Ritacco, and M. Reyes. Computer-assisted allograft selection for
2 transepiphyseal tumor resection at the knee. In: Proc. 10th Ann. Meet. CAOS-Int. 2010, pp. 91-
3 94.
- 4 5. Cohen J. A Coefficient of Agreement for Nominal Scales. *Educational and Psychological*
5 *Meas.* 20(1):37-46, 1960.
- 6 6. Delloye C., X. Banse, B. Brichard, P. L. Docquier, and O. Cornu. Pelvic reconstruction with a
7 structural pelvic allograft after re-section of a malignant bone tumor. *J. Bone Joint Surg. (Am)*
8 89A(3):579-87, 2007.
- 9 7. Delloye C., O. Cornu, V. Druetz, and O. Barbier. Bone allografts - What they can offer and
10 what they cannot. *J. Bone Joint Surg. (Br)* 89B(5):574-9, 2007.
- 11 8. Fleute M. and S. Lavallee. Building a complete surface model from sparse data using
12 statistical shape models: Application to computer assisted knee surgery. In: Proc. MICCAI 1998,
13 pp. 879-87.
- 14 9. Giannoudis P. V., H. Dinopoulos, and E. Tsiridis. Bone substitutes: an update. *Injury (Suppl 3)*
15 36:S20-7, 2005.
- 16 10. Hoeyer K. An anthropological analysis of European Union (EU) health governance as
17 biopolitics: The case of the EU tissues and cells directive. *Social Sci. Med.* 70(12):1867-73,
18 2010.
- 19 11. Landis J. R. and G. G. Koch. The measurement of observer agreement for categorical data.
20 *Biometrics* 33(1):159-74, 1977.
- 21 12. Matejovsky Z. Jr., Z. Matejovsky, and I. Kofranek. Massive allografts in tumour surgery. *Int.*
22 *Orthop.* 30(6):478-83, 2006.

- 1
2
3
4 1 13. Mizraji R., I. Alvarez, R. I. Palacios, C. Fajardo, C. Berrios, F. Morales, *et al.* Organ
5
6 2 donation in Latin America. *Transplant. Proc.* 39(2):333-5, 2007.
7
8
9 3 14. Mnaymneh W., T. I. Malinin, J. T. Makley, and H. M. Dick. Massive osteoarticular allografts
10
11 4 in the reconstruction of extremities following resection of tumors not requiring chemotherapy
12
13 and radiation. *Clin. Orthop. Relat. Res.* 4(197):76-87, 1985.
14
15
16 6 15. Muscolo D. L. , M. A. Ayerza, L. A. Aponte-Tinao, and M. Ranalletta. Partial epiphyseal
17
18 7 preservation and intercalary allograft reconstruction in high-grade metaphyseal osteosarcoma of
19
20 the knee. *J. Bone Joint Surg. (Am)* 86-A(12):2686-93, 2004.
21
22
23 9 16. Muscolo D. L. , M. A. Ayerza, L. Aponte-Tinao, and G. Farfalli. Allograft reconstruction
24
25 10 after sarcoma resection in children younger than 10 years old. *Clin. Orthop. Relat. Res.*
26
27 466(8):1856-62, 2008.
28
29
30
31 12 17. Ozger H., M. Bulbul, and L. Eralp. Complications of limb salvage surgery in childhood
32
33 13 tumors and recommended solutions. *Strategies Trauma Limb Reconstr.* 5(1):11-5, 2010.
34
35
36 14 18. Paul L., P. L. Docquier, O. Cartiaux, O. Cornu, C. Delloye, and X. Banse. Inaccuracy in
37
38 15 selection of massive bone allograft using template comparison method. *Cell Tissue Bank;*
39
40 9(2):83-90, 2008.
41
42
43 17 19. Paul L., P-L. Docquier, O. Cartiaux, O. Cornu, C. Delloye, and X. Banse. Selection of
44
45 18 massive bone allografts using shape-matching 3-dimensional registration. *Acta Orthopaedica*
46
47 81(2):252-7, 2010.
48
49
50 20 20. Paulussen M., S. Ahrens, J. Dunst, W. Winkelmann, G. U. Exner, R. Kotz, *et al.* Localized
51
52 Ewing tumor of bone: final results of the cooperative Ewing's Sarcoma Study CESS 86. *J. Clin.*
53
54 21 *Oncol.* 19(6):1818-29, 2001.
55
56
57
58
59
60
61
62
63
64
65

- 1
2
3
4 1 21. Rajamani K. T., M. A. Styner, H. Talib, G. Y. Zheng, L. P. Nolte, and M. A. Gonzalez
5
6 2 Ballester. Statistical deformable bone models for robust 3D surface extrapolation from sparse
7
8 data. *Med. Image Anal.* 11(2):99-109, 2007.
9
10
11 4 22. Ramseier L. E., T. I. Malinin, H. T. Temple, W. A. Mnaymneh, and G. U. Exner. Allograft
12
13 reconstruction for bone sarcoma of the tibia in the growing child. *J. Bone Joint Surg. (Br)*
14
15 5 88(1):95-9, 2006.
16
17
18 7 23. Ritacco L. E., A. E. Orias, L. A. Tinao, D. L. Muscolo, F. G. Bernaldo de Quirós, and I.
19
20 Nozomu. Three-Dimensional Morphometric Analysis of the Distal Femur: A validity method for
21
22 8 allograft selection using a virtual bone bank. In: Proc. 13th World Cong. Med. Health Inf. –
23
24 9 MedInfo 2010, pp. 1287-90.
25
26 10
27
28 11 24. Schmidt W., M. Reyes, F. Fischer, R. Geesink, L. P. Nolte, J. Racanelli, *et al.* Quantifying
29
30 12 human knee anthropometric differences between ethnic groups and gender using shape analysis.
31
32 In: Proc. Ann. Meet. Am. Soc. Biomech. 2009, pp. 26-29.
33
34 13
35
36 14 25. Seiler C., S. Weber, W. Schmidt, F. Fischer, N. Reimers, and M. Reyes. Automatic landmark
37
38 15 propagation for left and right symmetry assessment of tibia and femur: a computational anatomy
39
40 based approach. In: Proc. 9th Ann. Meet. CAOS-Int. 2009, pp. 195-198.
41
42
43 17
44
45 18
46
47
48 19
49
50 20
51
52
53 21
54
55 22
56
57
58 23
59
60
61
62
63
64
65

1
2
3
4
5
6
7
8
9
10
11
12
13
14
15
16
17
18
19
20
21
22
23
24
25
26
27
28
29
30
31
32
33
34
35
36
37
38
39
40
41
42
43
44
45
46
47
48
49
50
51
52
53
54
55
56
57
58
59
60
61
62
63
64
65

1 Figure 1. Processing Pipeline. (a) Original CT image. (b) Segmentation mask. (c) 3D
2 reconstruction of the tibiae and the tumor. (d) Cutting out the tumor in a virtual environment. (e)
3 Illustration of the similarity between the diseased bone and the mirrored version of the
4 contralateral tibia. (f) Illustration of how the template matching algorithm searches through the
5 virtual bone database. (g) Illustration of the good fit of a part cut out from the best batching tibia
6 and placed at the location of the resected section.

1
2
3
4 1 Figure 2. (Left) Mean surface distance (*MSD*) and (right) Hausdorff surface distance (*HSD*)
5
6 2 grayscale-coded maps illustrating the results of the validation protocol. The vertical axis
7
8 3 corresponds to the templates cut from the right tibiae, the horizontal axis corresponds to the left
9
10 4 bones of the 50 different subjects, and the origin lies in the upper-left corner. The low-intensity
11
12 5 diagonals correspond to distances measured for the contralateral bones of the same patient. Each
13
14 6 row corresponds to one simulated clinical case.
15
16
17
18
19 7
20
21 8
22
23 9
24
25
26 10
27
28 11
29
30
31 12
32
33 13
34
35
36 14
37
38 15
39
40
41 16
42
43 17
44
45 18
46
47
48 19
49
50 20
51
52
53 21
54
55 22
56
57
58 23
59
60
61
62
63
64
65

1
2
3
4 1 Figure 3. Three-dimensional view of a sample result. The surface distance between the template
5
6 2 cut from the right bone and the left tibiae from the databank is represented as color-coded surface
7
8 3 maps. The leftmost sample is the best match, the middle one is the second best, whereas the
9
10
11 4 rightmost bone is the bone that presented the highest *MSD*.
12
13
14
15
16
17
18
19
20
21
22
23
24
25
26
27
28
29
30
31
32
33
34
35
36
37
38
39
40
41
42
43
44
45
46
47
48
49
50
51
52
53
54
55
56
57
58
59
60
61
62
63
64
65

Figure1
[Click here to download Figure: figure1.eps](#)

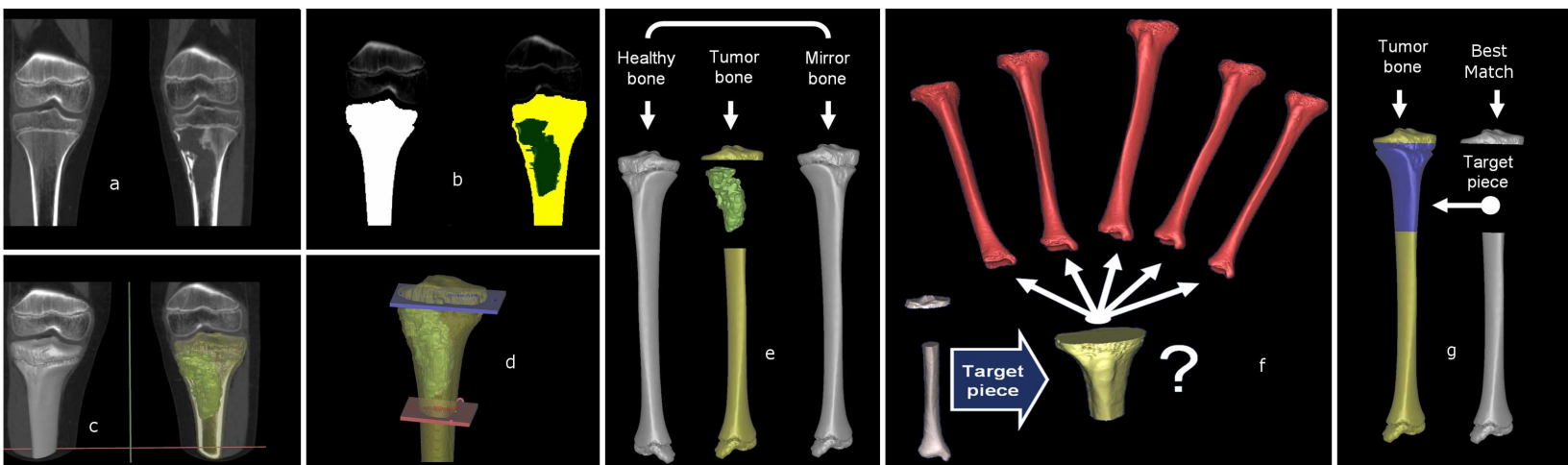


Figure2

[Click here to download Figure: figure2.eps](#)

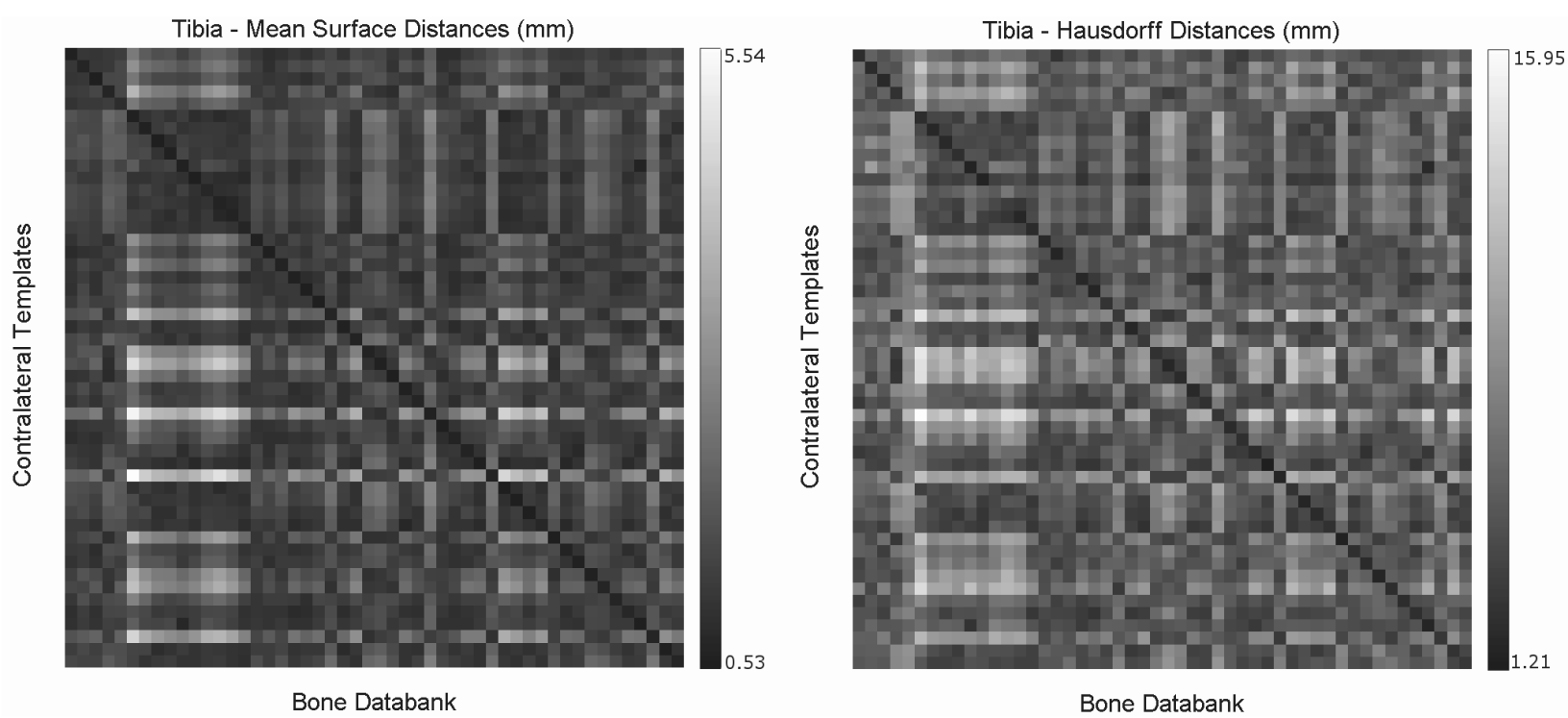
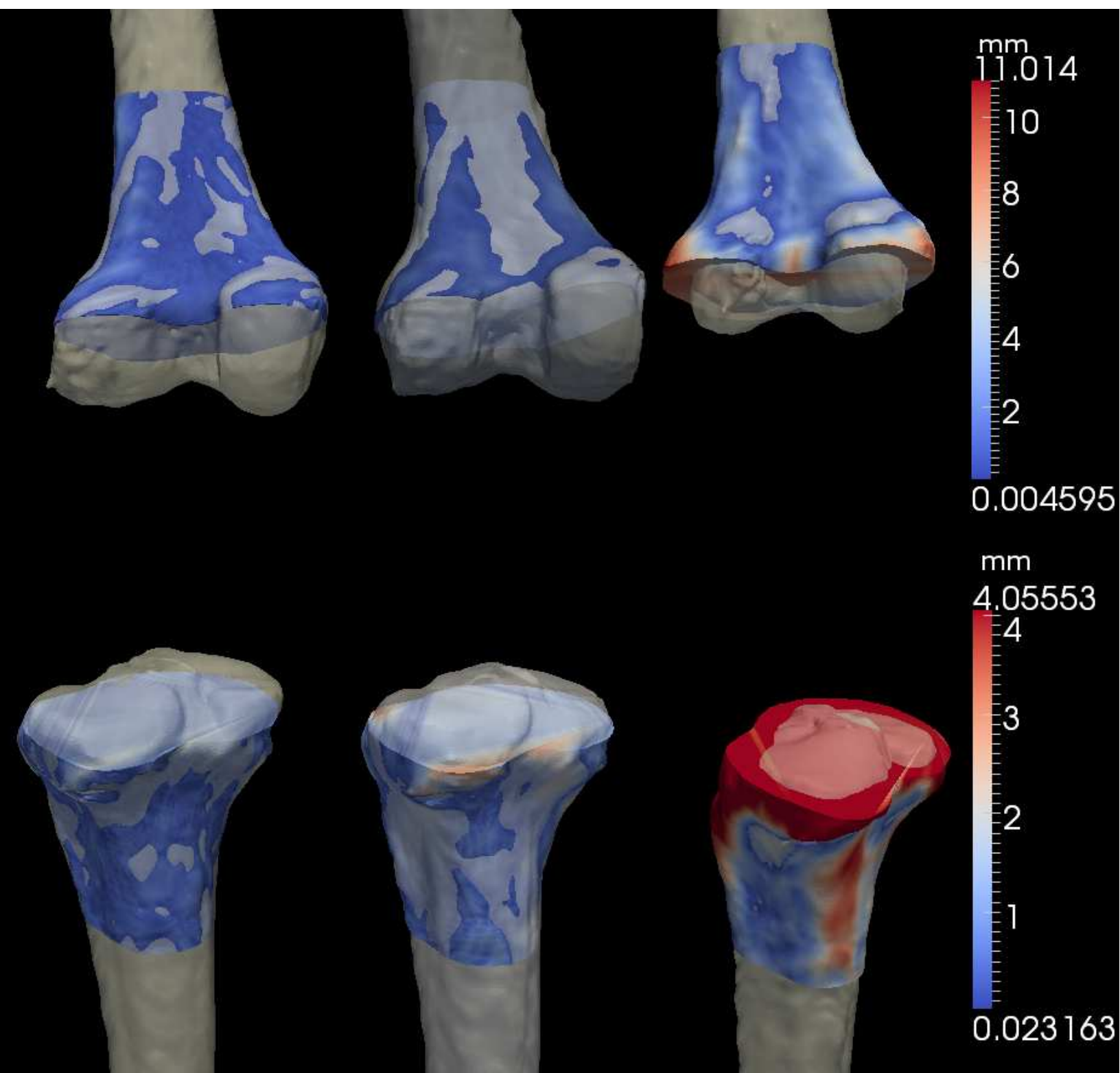


Figure3
[Click here to download Figure: figure3.eps](#)



Algorithm 1. Template Matching Algorithm

In: Search template s and all bones in the databank
 $DB = \{b_1, \dots, b_{\|DB\|}\}$

Out: Index of the closest matching bone in the databank
and the corresponding transformation parameters

```

1: Initialize  $j \leftarrow 0$ ;  $maxIt$ ;  $cc$ 
2: for each  $b_i$  in  $DB$ 
3:   loop
4:     find corresponding points
5:      $\mathbf{T}_j \leftarrow$  estimate updated parameters
6:      $s_T \leftarrow \mathbf{T}_j \circ s$ 
7:      $d_j \leftarrow MSD(s_T, b_i)$ 
8:     if  $(d_j - d_{j-1}) < cc \parallel j > maxIt$  then
9:        $D_i = \min\{d_k | k = 1 \dots j\}$ 
10:       $\mathbf{TR}_i = \mathbf{T}_{\text{argmin}\{d_k | k=1 \dots j\}}$ 
11:      break loop
12:     end if
13:      $j \leftarrow j + 1$ 
14:   end loop
15: end for
16:  $bestMatch \leftarrow \text{argmin}\{D_i | i = 1 \dots \|DB\|\}$ 
17:  $bestTransf \leftarrow \mathbf{TR}_{bestMatch}$ 

```

***Form for Disclosure of Potential Conflicts of Interest**

[Click here to download Form for Disclosure of Potential Conflicts of Interest: coi_disclosure.pdf](#)